Preliminary study on the transport of the nuclides in the secondary side of steam generator by using STAF code

CONG Tenglong[1,*], SU Guanghui[2], TIAN Wenxi[2], and QIU Suizheng[2]

1. *College of Nuclear Science and Technology, Harbin Engineering University, Harbin, 150001, China (tlcong@hrbeu.edu.cn)*
2. *State Key Laboratory of Multiphase Flow in Power Engineering, School of Nuclear Science and Technology, Xi'an Jiaotong University, Xi'an 710049, China*

Abstract: The steam generator tube rupture will result in the release of radioactive nuclides from primary coolant to second loop bypassing the vessel and containment. Prediction of the transport characteristics of nuclides can provide an insight of the distribution of radioactive particles in the shell side of steam generator. In this paper, the three-dimensional steam generator thermal-hydraulic analysis code STAF was employed to simulate the transport characteristics of nuclides in the steam generator shell side. The effects of leakage flow rate and leakage position on the distribution of nuclides are obtained. Leakage position changes the distribution of nuclides concentration significantly, while leakage flow rate only affects the absolute concentration values but does not impact the relative distributions.

Keyword: steam generator; thermal-hydraulic; nuclides transportation; STAF

1 Introduction

In the nuclear power plant, the steam generator (SG) plays a significant role as the primary-to-secondary side heat transfer boundary and also the role as the isolation between primary and secondary sides mass transfer. The SG tube thickness should be small to decrease the thermal resistance for a good heat transfer performance; however, thinner tube wall will reduce the structural strength of tubes. Besides, SG works in extreme severe environments, including the high pressure difference, chemical corrosion, mechanical vibration and so on, which may lead to the failure of SG heat transfer tube. The barrier to contain the radioactive products in the primary coolant will be disabled under the condition of SG tube rupture, and the contaminative substance will be released to the secondary loop, bypassing the reactor vessel and containment. Thus, it's essential to keep the integrity of SG tube under normal operation conditions and find out how the nuclides were transported in the shell side and determine the location of cracked tube under the SG tube rupture accident.

The integrity of SG tube is related to the situation of tube degradation caused by the fouling, corrosion, pitting and vibration, which depend on the localized three-dimensional thermal-hydraulic characteristics. A three-dimensional thermal-hydraulic analysis code, STAF, was developed and validated in our previous work [1, 2]. STAF code employed the porous media model to simplify the simulation of tube bundles with less computational cost and satisfactory accuracy and was used to the analysis of AP1000 SG [3] and the design of CAP1400 SG [4]. This code can predict localized three-dimensional thermal-hydraulic parameters for the primary and secondary sides of SG under the designed operated condition and low power conditions, including the velocity, pressure, vapor volume fraction and density. Besides, it can also provide key information for the analysis of flow-induced vibration of u-tube. Based on these, the STAF code can be used to improve the thermal-hydraulic and structural design of SG to reduce the risk of tube rupture.

However, there were still lots of SG tube rupture accidents reported in the past few decades. [5, 6] Two severe consequences will be caused by the tube rupture. The first one is the increase of shell side inventory. The water level in SG secondary side will rise with increasing the inventory, thus, the separators may be immersed by the two-phase mixture. The two-phase mixture with high humidity will flow into the main steam line without being separated, resulting in the failure of turbine. The water level increase caused by tube rupture used to be analyzed

Received date: April 17, 2017
(Revised date: May 22, 2017)

by using the one-dimensional system code since this calculation is depend on the leak rate, the mass balance in the shell side of SG and the operation condition of the secondary loop. Thus, the three-dimensional characteristics do not affect the accuracy very much. Besides, three-dimensional code cannot capture the system response since it only models the SG. The other consequence is the release of radioactive substances from primary to secondary coolants. This release of radioactive products will contaminate the shell side fluid and can be determined through the SG blowdown system with the chemical sampling. However, the distribution of nuclides and the location of the rupture cannot be determined until the reactor shutdown and operator can get a view into the SG. The radioactive nuclides released from the different rupture locations show different concentration distributions in the shell side of SG. Thus, the operator may find the possible location of tube rupture with a deep insight of the three-dimensional nuclide distributions released from certain locations.

In this work, the STAF code was updated by adding the concentration transport equation to model the distribution of radioactive nuclides in the SG secondary side. The localized thermal-hydraulic characteristics as well as the nuclides concentration can be obtained by using the updated STAF code. Besides, the effects of rupture locations on the distribution were obtained for a better understanding of the nuclides transport characteristics.

2 Mathematical models

The mathematical models employed in the original STAF code include the conservation equations for the primary side fluid, conservation equations for the secondary side fluid, primary-to-secondary side heat transfer equation and the constitutive equations. In this work, the updated STAF code also solves the nuclide transport equation to get the nuclides distribution. These models are briefly introduced in this section.

2.1 Primary side governing equations

The primary side flow is simplified as the single phase flow through multi-channel. The primary side fluid is assumed to be incompressible. The mass flux distribution in all tubes is calculated by the pressure balance between the inlet and outlet plenums. The tubes are divided into small sections based on the secondary side grids. The pressure balance equation for each tube is

$$\sum_i \Delta p_i = p_{in} - p_{out} \tag{1}$$

where Δp_i is the total pressure drop in the i th section in a certain tube; p_{in} and p_{out} are the pressure in the inlet and outlet plenums. The energy conservation equation for tube sections in each secondary side calculation mesh is

$$\sum_j \left[A_c \left(v_{p,in} \rho_{in} c_{p,in} T_{in} - v_{p,out} \rho_{out} c_{p,out} T_{out} \right) \right]_i = q_A A_s \tag{2}$$

where A_c, v_p, ρ, c_p, T, q_A, and A_s are the flow area in tubes, primary side velocity, density of primary side coolant, temperature of primary side fluid, heat flux at the outer surface of tube and the total outer surface area of tube sections in a secondary side calculation mesh, respectively. The subscripts *in* and *out* mean the inlet and outlet of tube section. The subscript *j* denotes the j th tube section in a secondary side calculation mesh.

2.2 Secondary side governing equations

In the secondary side of SG, coolant is heated from single-phase liquid to two-phase mixture. In the STAF code, the drift flow model is employed to solve the localized thermal-hydraulic parameters. The control equations for two-phase flow through porous media are given as following.

Continuity equation:

$$\nabla \cdot \left(\beta \rho_m \vec{v_m} \right) = 0 \tag{3}$$

Momentum equation:

$$\nabla \cdot \left(\beta \rho_m \vec{v_m} \vec{v_m} \right) = -\beta \nabla p + \nabla \cdot \left(\beta \mu_{m,eff} \nabla \vec{v_m} \right) + \beta \rho_m \vec{g} + \nabla \cdot \left(\frac{\beta \alpha_g \rho_g}{\left(1-\alpha_g\right)\rho_l} \rho_m \vec{v_{gm}} \vec{v_{gm}} \right) + S_{\vec{v}} \tag{4}$$

Energy equation:

$$\nabla \cdot \sum_{k=1}^{2} \left(\beta \alpha_k \vec{v_k} \left(\rho_k E_k + p \right) \right) = \nabla \cdot \left(\beta k_{eff} \nabla T \right) + S_E \tag{5}$$

Void fraction equation:

$$\nabla \cdot \left(\beta \alpha_g \rho_g \vec{v_m} \right) = -\nabla \cdot \left(\beta \alpha_g \rho_g \vec{v_{gm}} \right) + S_g \tag{6}$$

where, β is the ratio of volume occupied by fluid and total volume in a control volume, calculated by the geometry calculation module; α_g is the volume fraction of vapor phase; ρ_m and ρ_g are the densities of mixture and vapor, respectively; $\vec{v_m}$ and $\mu_{m,eff}$ are the velocity and effective viscosity of mixture

phase, respectively; p is the pressure; E is the internal energy; k_{eff} is the effective conductivity; $\overrightarrow{v_{gm}}$ is the drift velocity of vapor phase relative to the mass-weighted average velocity of the two-phase mixture; the subscript k stands for liquid and vapor for k equals to 1 and 2, respectively. S_v is the additional momentum source term employed to consider the resistances of downcomer, tube bundle, separators as well as support plates. S_E is the energy source to present the energy transfer between primary and secondary side fluid. S_g is the mass source for vapor phase.

The nuclides transport equation is added into the STAF code to predict the concentration distribution of radioactive products released from the primary side. In the STAF code, the radioactive substances are assumed only dissolved in the liquid phase. Thus, the control equation for the nuclides can be written as

$$\nabla\cdot\left(\beta\alpha_l\rho_l\overrightarrow{v_m}Y\right)=-\nabla\cdot\left(-\beta\alpha_l\rho_l D\nabla Y-D_T\frac{\nabla T}{T}\right)+S_n \quad (7)$$

where ρ_l is the liquid density, kg/m^3; Y is the nuclide concentration, kg/m^3; D is the mass diffusion coefficient, m^2/s; D_T is the thermal diffusion coefficient, kg^2/m^4/s; and S_n is the source term to present the leaked nuclides, kg^2/m^6/s.

The turbulence of two-phase flow in porous media was calculated by using a validated zero-quation model, which is

$$\mu_{eff}=C\rho_m w_m l \quad (8)$$

where C is a constant; w_m is the mixture velocity along the tube; l is the characteristic length.

2.3 Primary-to-secondary side heat transfer equation

The primary-to-secondary side heat flux is calculated by

$$q_A=\left(T_p-T_s\right)\times\left(\frac{1}{h_p}+\frac{\delta}{k}+R_{foul}+\frac{1}{h_s}\right)^{-1} \quad (9)$$

where $T_p, T_s, h_p, \delta, k, R_{foul}$ and h_s are the primary side temperature, secondary side temperature, primary side heat transfer coefficient, tube thickness, tube conductivity, fouling resistance and secondary side heat transfer coefficient, respectively. q_A is the heat flux at tube outside wall, which is associated with S_E in Eq. (5) by

$$S_E=q_A A_{SV} \quad (10)$$

where A_{SV} is the tube outer surface area concentration, *i.e.*, the area wetted by secondary side fluid per unit volume.

2.4 Constitutive equations

The constitutive equations include equations for flow resistance, heat transfer, boiling mass transfer, turbulence and drift velocity, which can be found in our previous work [1].

3 Grid strategy, boundary conditions and numerical scheme

The STAF code contains the models for downcomer, tube bundle, tube support plates and separators. The tube bundle is descripted by using the porous media model, while the tube support plates are presented by the porous jump boundary with given flow resistance coefficients. The separators are transformed into trapezoid or rectangle channels with channel centers and flow areas equal to the prototype circular channels. Besides, STAF code just takes into account the flow resistance of separators without considering the vapor-liquid separation effects. The geometry and the grid strategy are given in Fig. 1. This domain is discretized by using about 0.11 million hexahedral cells.

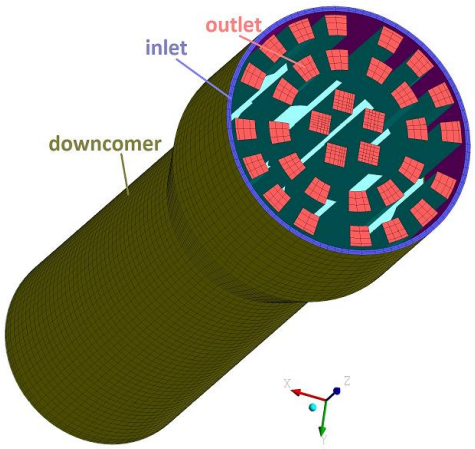

Fig. 1 Geometry and grid for AP1000 SG.

Boundary conditions should be set to determine the definite solution of differential equations. For the shell side, the inlet and outlet are located on the up surfaces of downcomer and separators, with uniform inlet velocity and outlet pressure, respectively. The inlet boundary conditions, including temperature and velocity are calculated based on the feedwater

temperature and mass flow, recirculation water mass flow, system temperature and geometry. The outlet pressure is set as the plenum pressure. The inlet and outlet boundary conditions of primary side fluid are mass flow inlet and fully developed outflow, respectively. Details for all the boundary conditions are presented in Table 1.

Table 1 boundary conditions

domains	boundary locations	boundary types	values
secondary side	operating pressure		5.64 MPa (equals to the plenum pressure)
	inlet	velocity inlet	liquid phase2.66 m/s vapor phase 0 m/s vapor phase void fraction 1.0×10^{-10}
		temperature	533.13 K
	outlet	pressure outlet	0 Pa (relative to operating pressure)
primary side	inlet	mass flow rate	7151.4 kg/s
		temperature	594.15 K
	outlet	outflow	-

As for the SG tube rupture, the leak positions, the leak flow rate and the nuclide concentration are parameters of interests. In an in-service power plant, many nuclides are generated in or injected into the reactor core and dissolved in the primary coolant, including the boron, lithium, sodium, iodine and xenon [7]. The transport characteristics of all these nuclides are similar. In this work, the transport of lithium is studied. In the normal operating period, the concentration of lithium varies from 0.2 to 3.5 ppm. The lithium concentration in primary coolant is set as 3.0 ppm. Two leak flow rates are investigated to analyze the effects, which are 5 kg/s and 13 kg/s [8]. Besides, twelve possible leak positions are designed for the location sensitive study, as shown in Fig. 2. These twelve positions locate at three planes with different heights, presenting the locations near the bottom, in the middle and near the roof of straight tubes. The mass, momentum and energy equations are solved prior to the nuclide transport equation to obtain an initial thermal-hydraulics distribution, and then the nuclide transport equation as well as all other three governing equations are solved to reach the final solution. This calculation procedure (as shown in Fig. 3) can help to reach a better convergence performance.

4 Results and discussions

In this work, a steady simulation is performed to study the nuclides distribution by using a three-dimensional code. As can be found in the boundary condition and the numerical method, the effects of leakage flow rate on the water level cannot be predicted by STAF since it supposes a given secondary inlet flow rate and outlet pressure. The effects of pressure balance on the water level cannot be taken into account by using this code. Actually, STAF code does not focus on the predict of transient water level under the situation of changing working conditions, such as power transient or LOCA condition, since this code is developed to predict the localized three-dimensional thermal-hydraulic characteristics, which are essential for the design and structural integrity. In the hypothetical SG tube rupture scenarios, the leakage flow rate is quite small when compared to the total secondary mass flux (13 kg/s v.s. 3497 kg/s), the leakage flow will only effects a small region close to the leakage position. The resultant general thermal-hydraulic parameters are quite similar to these under the normal operating condition. In this section, the thermal-hydraulic characteristics are presented briefly and the main interests are focused on the characteristics related to the nuclides distribution.

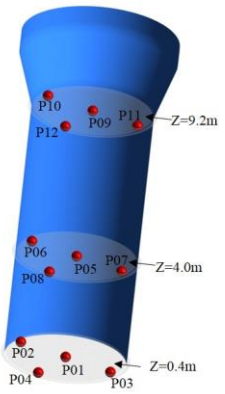

	x/m	y/m	z/m
P01	0	0	0.4
P02	1.7	0	0.4
P03	-1.7	0	0.4
P04	0	1.7	0.4
P05	0	0	4.0
P06	1.7	0	4.0
P07	-1.7	0	4.0
P08	0	1.7	4.0
P09	0	0	9.2
P10	1.7	0	9.2
P11	-1.7	0	9.2
P12	0	1.7	9.2

Fig. 2 Hypothetical leak positions.

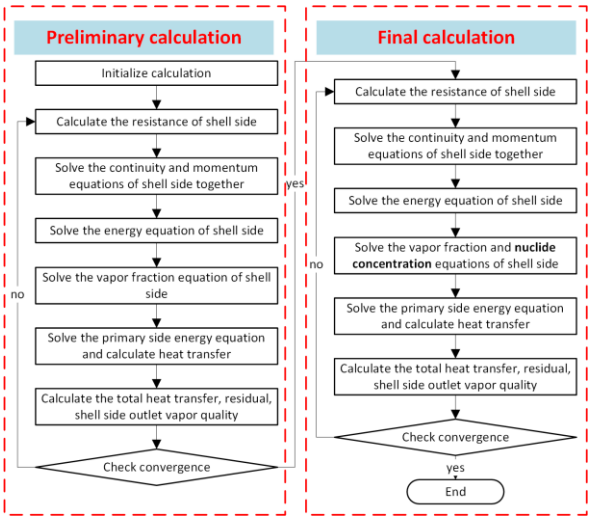

Fig. 3 Calculation procedure.

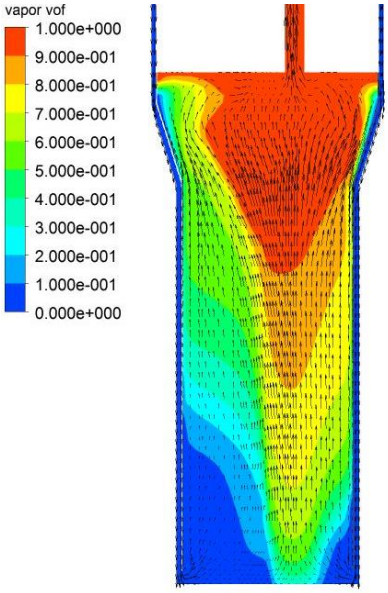

Fig. 4 Vapor volume fraction and velocity vector at the symmetric plane.

The vapor volume fraction at symmetric plane is given in Fig. 4. As can be seen, the vapor fraction increases from zero at the bottom to more than 90 percent in the elbow region. Besides, the vapor fraction in hot side is much larger than that in cold side, which is because more than 2 times of heat is released in hot side than that in cold side due to the temperature difference in primary side. Moreover, the velocity vectors are also shown in Fig. 4. Two-phase mixture flows faster in hot side than in cold side due to the lower density and higher energy density in hot side. The cross flow near tubesheet is considerable, while it's negligible in other part of the straight tube region. However, the velocity vectors become complicated in the elbow region and the region above it due to the influences of u-tubes and separators, which will lead to a dispersion in the nuclides distribution.

Figure 5 presents the distribution of lithium concentration released from different locations with a constant leakage rate of 13.0 kg/s. As can be seen, in general, the nuclides do not diffuse too much in the straight tube region, which means the nuclides just entrainment upwards with the two-phase mixture. However, the nuclides disperse into a large region in the elbow tube region, which may due to the increase of cross flow caused by the u-bend and the separators. Besides, the vaporization of liquid phase will also increase the nuclides concentration due to the assumption that nuclides only dissolved in the liquid phase. The concentration in the elbow region may increase to ten times of that in the bottom region since the vapor volume fraction increases from zero to a value larger than 90 percent. Moreover, the maximum nuclide concentration for most cases are less than 10 ppm, except cases P09 and P12, where the leakage positions are at the center and the left side of symmetric plane. This is because the leakage locates in the region where vapor volume fraction is larger than 90 percent and the nuclide is assumed to be only dissolved in the liquid phase.

Figure 6 shows the streamlines emitted from the leakage positions for all these 12 cases. As can be seen, the streamlines do not spread too much, especially these emitted from the middle and up planes. Nevertheless, the streamlines from P02, P03 and P04 spread out in the radial direction due to the strong cross flow in the region near the bottom of tubes, which leads to the fan-shaped distribution of nuclides in these cases (Fig. 5 b-d), since the transport caused by diffusion effects are quite weak compared to that caused by convection. Besides, the streamlines of P09-P12 are still bunched even in the elbow region where cross flow velocity is large, demonstrating that the dispersed nuclide distribution in the u-bend region shown in Fig. 5 is not caused by the convection, but by the liquid evaporation. What's more, the nuclide density on the symmetric plane is given in Fig. 7 to show the absolute concentration (concentration in liquid phase multiple by liquid volume fraction) of nuclide distribution for case P10

and P11. As can be seen, the transport of nuclide follows the direction of velocity vectors and the dispersion zone of nuclides distribution is much smaller than that shown in Fig. 5. This means, most of the nuclides are escaped with fluid flowing out from the separators.

The effects of leakage flow rate on the distribution of nuclides are shown in Fig. 8. As can be noted, the streamlines released from the leakage positions are almost same for these two leakage flow rate. The high concentration regions fit well with the streamlines, which proves that the transport of nuclides is governed by the convection. The diffusion of nuclides disperses the particles in the transversal direction, but the concentration diffused to the center of SG is quite lower compared to the concentration transported by the convection. Besides, the released nuclides dispersed in a similar way with analogous concentration distribution shapes. However, the values of the concentration are quite different. In the case with 13.0 kg/s leakage rate, the maximum concentration is 0.99 ppm, while it reduces to 0.38 ppm for the case with 5.0 kg/s leakage rate. Besides, it can be observed from the contour lines that the relative nuclides concentrations distribute in the same shape even though the absolute values of concentrations differ a lot.

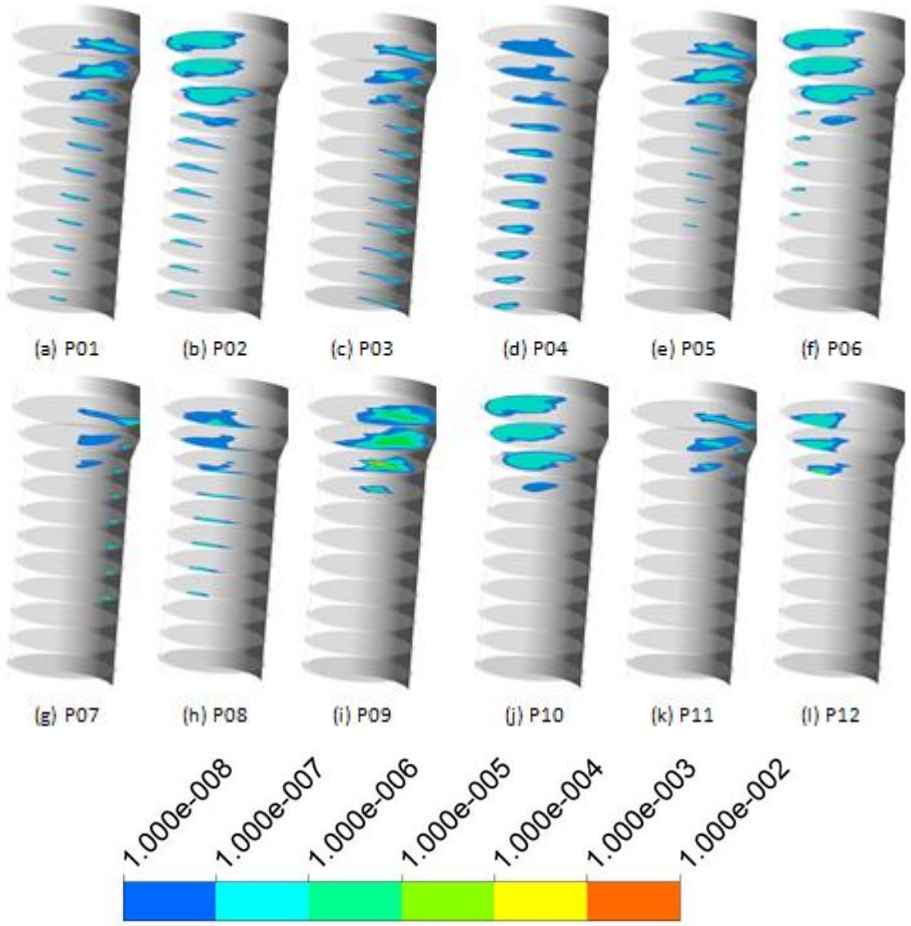

Fig. 5 lithium concentration distribution released from different positions.

Table 2 gives the total lithium inventory in the shell side of SG. As can be seen, the inventory varies significantly with the leakage position and leakage flow rate. The maximum lithium inventory appears when the nuclides leaked from the center of z=9.2m plane. Besides, the inventories leaked from the hot side (cas02, cas06, cas10 and cas13) are lower than these from the cold side (cas3, cas07, cas11 and cas14) and the difference between these cases decrease with increasing the leakage height and decreasing the leakage flow rate. This is because of the differences in velocity and vapor volume fraction in the hot and cold sides. In the hot side, the mixture velocity is much higher than that in the cold side due to the larger vapor volume fraction. Thus, the inventory of lithium can be removed from the SG

shell side efficiently, even though the concentration distribution in liquid phase of hot side is much larger than that of cold side (as shown in Fig. 5)

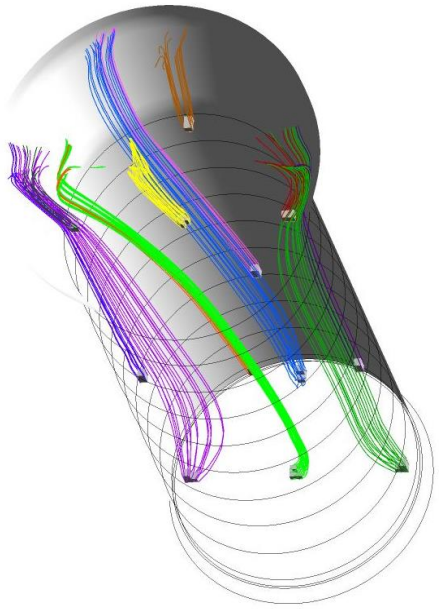

Fig. 6 Streamlines emitted from the leakage positions.

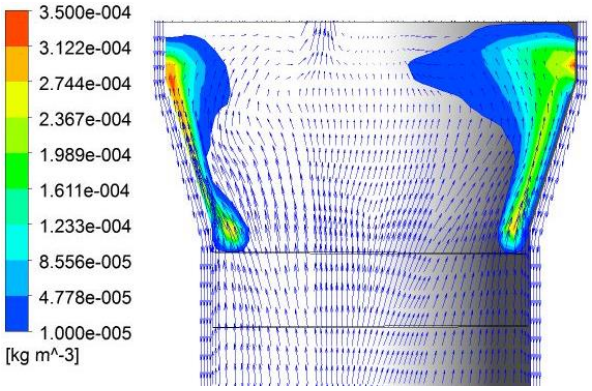

Fig.7 Nuclide density on the symmetric plane (value clipped to 1.0e-5 to 3.5e-4).

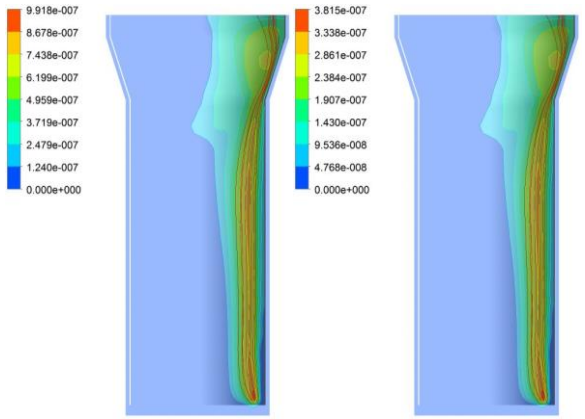

(a) cas02, P02, 13kg/s (b) cas13, P02, 5kg/s

Fig. 8 Effects of leakage flow rate on the distribution of nuclides concentration.

5 Conclusions

In this paper, the STAF code is updated to predict the transport characteristics of nuclides released from the primary coolant in a SG tube rupture scenario. The effects of leakage flow rate and leakage position on the nuclides distribution are analyzed. Following conclusions can be obtained.

1) The updated STAF code can be used to predict the three-dimensional nuclides distribution.
2) The effects of leakage flow rate and leakage position on the three-dimensional thermal-hydraulic characteristics are quite small.
3) The nuclides distributions and nuclides inventory in SG vary with the leakage positions significantly, while the leakage flow rate does not affect the relative distribution of nuclides.

Table 2 Total lithium inventory in SG

Case No.	Leakage position	Leakage flow rate (kg/s)	Total lithium inventory in SG (g)
cas01	P01	13.0	0.401
cas02	P02	13.0	0.385
cas03	P03	13.0	0.768
cas04	P04	13.0	0.482
cas05	P05	13.0	0.312
cas06	P06	13.0	0.303
cas07	P07	13.0	0.439
cas08	P08	13.0	0.311
cas09	P09	13.0	1.335
cas10	P10	13.0	0.146
cas11	P11	13.0	0.147
cas12	P12	13.0	0.165
cas13	P02	5.0	0.148
cas14	P03	5.0	0.295

References

[1] CONG, T., ZHANG, R., TIAN, W., QIU, S, and SU, G.: Development and preliminary validation of a steam generator 3D thermohydraulics analysis code STAF, Nuclear engineering and design, 298 (2016) 135-148.

[2] CONG, T., ZHANG, R., TIAN, W., SU, G., and QIU, S.: Analysis of Westinghouse MB2 test using the steam-generator thermohydraulics analysis code STAF, Annals of Nuclear Energy, 85 (2015) 127-136.

[3] CONG, T., TIAN, W., QIU, S, and SU, G.: Study on secondary side flow of steam generator with coupled heat transfer from primary to secondary side, Applied Thermal Engineering, 61 (2013) 519-530.

[4] CONG, T.: Research on Thermohydraulics Characteristics in Steam Generator of the Large

Advanced PWR. Xi'an, China: Xi'an Jiaotong University, 2016.

[5] BANIC, M., BROS, J., CIZELJ, L., CORNET, P., DRAGUNOV, J., FLUCKIGER, G., GOLD, R., ITO, N., MACDONALD, P.E., and MARUSKA, C.: Assessment and management of ageing of major nuclear power plant components important to safety: Steam generator, in, International Atomic Energy Agency, Vienna, Austria, 1996.

[6] MACDONALD, P.E., SHAH, V.N., WARD, L.W., and ELLISON, P.G.: Steam generator tube failures, in, Nuclear Regulatory Commission, Washington, DC, US, 1996.

[7] DONG, S., GUO, W., SHAN, S., XU, W., and TIAN, L.: AP1000 Nuclear Power English Textbook, CNNC Sanmen Nuclear Power Co. Ltd., Zhejiang, China, 2010.

[8] FERNG, Y.: Investigating the distribution characteristics of boiling flow and released nuclide in the steam generator secondary side using CFD methodology, Annals of Nuclear Energy, 34 (2007) 724-731.